Distributed Bragg reflectors for the colorimetric detection of bacterial contaminants and pollutants for food quality control

Giuseppe M. Paternò (ID), Giovanni Manfredi (ID), Francesco Scotognella (ID), and Guglielmo Lanzani (ID)

View Online   Export Citation   CrossMark

Distributed Bragg reflectors for the colorimetric detection of bacterial contaminants and pollutants for food quality control

Giuseppe M. Paternò,[1] [iD] Giovanni Manfredi,[1] [iD] Francesco Scotognella,[1,2] [iD] and Guglielmo Lanzani[1,2,a] [iD]

AFFILIATIONS

[1] Center for Nano Science and Technology, Istituto Italiano di Tecnologia (IIT), Via Pascoli 10, 20133 Milano, Italy
[2] Physics Department, Politecnico di Milano, Piazza L. da Vinci 32, 20133 Milano, Italy

[a] Author to whom correspondence should be addressed: Guglielmo.lanzani@iit.it

ABSTRACT

Real-time monitoring of bacterial contaminants and pollutants in food is of paramount importance nowadays, owing to the impressive extension of the food production/supply chain and the consequent increase in foodborne outbreaks worldwide. This represents a serious risk for consumers' health and accounts for a large fraction of food wastage, especially in the developed countries. Therefore, modern sensors for food quality control should possibly afford low-cost, portability, and easiness of readout to enable widespread diffusion of the technology, thus allowing food quality monitoring from the production/supply chain to the consumers' table. In these regards, one-dimensional photonic crystals, also known as Distributed Bragg Reflectors (DBRs), can represent simple yet efficient all-optical and label-free colorimetric sensors, given their relatively high color purity, easiness of integration with a large number of stimulus responsive materials, and low-cost fabrication from scalable processes. In this perspective article, we discuss the development of DBRs-based colorimetric sensors for the monitoring of bacterial contaminants and pollutants of interest in the food quality sector. We aim at providing a systematic overview on the main approaches that have been employed to achieve selectivity and sensitivity in DBRs-based sensors, with the view to enable widespread use of this technology at both the industry/supply chain and customers' level.

I. INTRODUCTION

The relentless world population growth comes along with the massive extension of food production and supply chain worldwide. This, however, can pose serious risks for food quality, especially for those goods that can easily degrade (i.e., meat, fresh fruits, and vegetables). Accordingly, the field of sensing for food quality control is expanding at utmost rate.[1–3] Food contamination brings a number of serious risks for consumers' health and contributes to an increase in wastage. Its prevention and mitigation is, therefore, a top priority in reducing food waste and can be seen as an active and important part of a well-developed circular economic system.[4] In particular, it has been estimated that one third of the food produced around the world is wasted ($\sim 1.3 \times 10^9$ tons per year),[4] and a large part of this wastage originates from food contamination in developed countries (e.g., in the USA). Hence, given the increasing number of

pathogen-outbreaks in food, the need for simple, cost-effective, and portable sensing devices has become paramount both at the industry/supply chain and at the customers' level, within the new circular economy paradigm.[5]

In this context, a plethora of methods and techniques have been proposed and utilized for tracking food contaminants and/or by-products of the degradation process.[6,7] Apart from traditional colony counting (i.e., for bacterial pathogens), immunological assays, and polymerase chain reaction (PCR)-based methods that despite their relatively high sensitivity usually suffer from low turn-around time for results, new bio-sensing methods involving optical interrogation of the contaminated samples hold great promise for rapid and low-cost detection of common contaminants. These include vibrational spectroscopies (Raman and Fourier-transform infrared spectroscopies), detection of surface plasmon resonance, optical fibers, and resonators,[8] among others. However, all these

approaches are stacked at a low technology readiness level, for they rely on the use of expensive equipment and specialized personnel, hampering a widespread use of the technology. Indeed, modern biosensors shall provide a simple and rapid readout that can be analyzed even by unskilled operators. For instance, large availability of simple and low-cost bio-sensors can be of vital importance in developing countries, as well as in rural area of the developed world, due to the lack of infrastructure and specialized personnel.

Driven by the possibility to build up miniaturized and cheap devices, photonic crystals (PhCs) have emerged recently as a promising class of (bio)sensing platforms mostly due to two reasons: first, the versatility in terms of fabrication and functionalization,[9] and second, the ease of detection, by naked eye, based on the change in the color. PhCs can be considered as an assemblage of periodically arranged materials with different dielectric functions in 1D, 2D, or 3D, in which only certain wavelengths of light, set by the periodic spacing (d), can propagate through the structure [Fig. 1(a)]. This in turn leads to the generation of structural colors[10,11] that emerge without the presence of pigments, an effect widely found in nature.[12,13] The well-known phenomenon of x-ray reflection [Fig. 1(b)] can be roughly adapted to explain the reason why PhCs reflect light of certain wavelengths. In the case of x-ray diffraction, only those beams positively interfering with each other produce regular oscillations (Bragg's reflections) that are characteristic of the interplanar distance d and incidence angle θ, in agreement with the Bragg's law $2d\cos\theta = m\lambda$. If we combine Bragg's law with Snell's law, introducing the effective refractive index (RI) of a two-material repetitive unit (n_{eff}), we obtain the Bragg–Snell law (see equation in Fig. 1), which links the interplanar distance and the refractive indices of the PhCs to the wavelengths of reflected light, the so-called photonic bandgap (PBG). From these expressions, one can easily infer that the structural color of PhCs can be sensitive to a number of environmental effects and stimuli that modulate the refractive index contrast and the lattice spacing, therefore enabling application of PhCs in sensing. In order to enhance the analyte interaction with the photonic lattice and cause an effective modulation of the photonic bandgap and, hence, the structural colors, most PhC-based sensors exploit porosity in the architecture or permeability of the components. Both strategies rely on the notion that n_{eff} is a spatial average affected by infiltration of the analytes in the PhC structure and that infiltration may also change the PhC periodicity due to swelling or shrinking of the architecture geometry. Unskilled operators can easily assess the consequent color changes by a quick visual inspection of the PhC as long as the variation is higher than the wavelength discrimination threshold, which is often below 50 nm even for people suffering from color deficiency.[14] Nature offers many examples to validate this idea, for instance, the wings of Morpho rhetenor butterfly are natural PhCs.[10] When ethanol is added on the wings, in fact, one can observe an evident color shift [Fig. 1(d)] that originates from the change in the effective refractive index after infiltration of the liquid inside the microstructure.[13,15,16]

One-dimensional PhCs, also known as Distributed Bragg Reflectors (DBRs) or Bragg stacks, represent the simplest photonic architecture as the bandgap simply originates from the alternation of layers with different refractive indices. The intrinsic simplicity of DBRs and their well-defined optical features, relatively easy fabrication, and compatibility with a variety of stimulus responsive functionalities[18–20] have enabled their use as versatile detection platforms.[9,21–23] Figure 1(d) reports the typical optical response of a DBR with the characteristic reflectivity peak centered at E_{PBG} with a ΔE_{PBG} width, while the inset in Fig. 1(d) represents the

$$2d(n_{eff}^2 - \sin^2\theta)^{1/2} = m\lambda$$
$$n_{eff}^2 = n_H^2 V_H + n_L^2 V_L$$
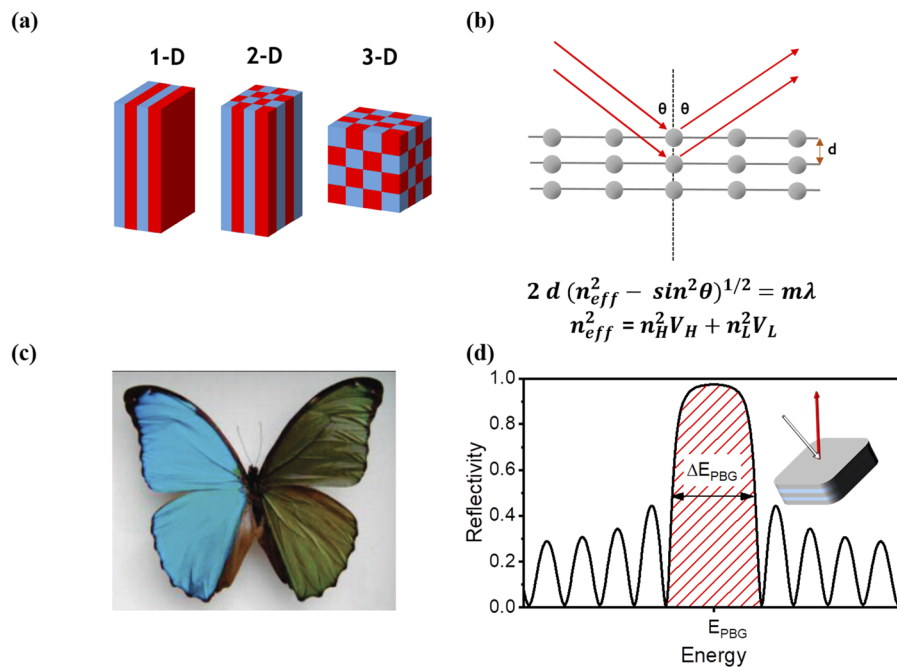
FIG. 1. (a) Schematic representation of 1D, 2D, and 3D PhC architectures. (b) Scheme of light reflection mechanism in PhCs. (c) Picture of the wings of Morpho rhetenor upon addition of ethanol on the right wing [Adapted from R. A. Potyrailo, Proc. SPIE (2011). Copyright 2011 Society of Photo-Optical Instrumentation Engineers (SPIE).][17] (d) Typical reflectivity of a Distributed Bragg Reflector (DBR). The PBG region, which is centered at E_{PBG} and ΔE_{PBG} wide, is denoted by the red patterned area. The inset shows the structure of the DBR, composed of alternated layers of materials having two different refractive indices.

structure of a DBR composed of alternated layers of two different materials exhibiting different refractive indices. The exact position of the bandgap in wavelength (λ_{PBG}) can be calculated by means of the following expression:

$$\lambda_{PBG} = 2D\sqrt{n_{eff}^2 - \sin^2\theta}, \tag{1}$$

where D is the total thickness of the repetitive unit and n_{eff} is the effective refractive index of each double layer ($n_{eff} = \frac{n_H d_H + n_L d_L}{d_H + d_L}$, where n_H and n_L are the highest and lowest refractive indices of the material pair, respectively, while d_H and d_L are the thicknesses of the respective layers). The energetic width of the bandgap instead follows

$$\Delta E_{PBG} = \frac{4E_{PBG}}{\pi}\frac{n_H - n_L}{n_H + n_L} = \frac{4E_{PBG}}{\pi}\frac{\Delta n}{2n_L + \Delta n}, \tag{2}$$

while the maximum reflectivity intensity follows

$$R_{PBG} = 1 - 4\left(\frac{n_L}{n_H}\right)^N = 1 - 4\left(1 - \frac{\Delta n}{n_H}\right)^N. \tag{3}$$

All those above-mentioned expressions indicate that the reflectivity output of a DBR is strongly connected to the refractive environment, allowing one to track the presence of analytes by simply analyzing the photonic bandgap peak position, intensity, and angular dispersion. For instance, Fig. 2 displays two color-coded maps showing the changes in reflectivity due to swelling/shrink of the multilayer and changes in the high refractive index layer. The thickness variation [Fig. 2(a)] induces a rigid shift of the reflectivity energy response following a linear relation with the thickness, as a direct consequence of the electromagnetism law scale invariance.[24] The modulation of the refractive index instead results in a more convoluted behavior [Fig. 2(b)]. In particular, while we can still observe a shift of the PBG due to the shrinkage of the optical path upon an increase in the refractive index, the consequent increase in the contrast Δn causes an enhancement of the reflectivity intensity and a broadening of the PBG, in agreement with Eqs. (2) and (3). Note that at lower n_H values, when the high index gets near n_L, the PBG almost disappears as the material is virtually homogeneous and, hence, does not show any photonic effect, with the exception of the appearance of weak interference fringes.

While sensing can be based on similar phenomena as reported above, it is worth noting that those variations are typically not analyte-selective; therefore, various methods have been proposed to achieve selectivity. In addition, such sensors should aim at a full colorimetric response that would enable an effective wide spreading of the technology.

In this perspective article, we will provide an overview of the main approaches employed to confer DBR's selective responsivity with respect to common bacterial contaminants and pollutants of interest in the field of food quality control and introduce our view on the development of this branch of research that holds great promise for the development of simple colorimetric sensing devices.

II. MESOPOROUS DBRs

Porosity at the mesoscale level can be considered a simple yet effective responsivity element in DBRs. This provides already two useful functionalities, namely: (i) a porous structure that allows percolation and accommodation of liquids and capillary condensation of vapors within the air voids, thus determining a modulation of the refractive index contrast; (ii) a relatively large surface area, which is required for efficient chemical/physical functionalization of the inner part of the DBR, i.e., for biorecognition purposes. The first seminal works on porous DBRs obtained by electrochemical etching of silicon (porous silicon, PSi) were reported two decades ago[25–28] and have paved the way for their utilization in a range of applications, such as lasing,[17] chemical sensing,[30,31] and biosensing.[32–34] Within the context of PSi-based DBRs, the majority of reports exploit an optical resonator configuration, composed of a Fabry–Perot microcavity integrating emissive materials (i.e., silicon nanocrystals) embedded between two DBRs. The interaction between the analyte and the proper chemical functionality decorating the microcavity leads to a shift of the emission peak, which is modulated and narrowed down by the microcavity. Such an architecture permits attaining a relatively high sensitivity, as tiny changes in the effective optical thickness modify the reflectivity spectrum, causing a spectral shift in the interference pattern.[35] For instance, this approach has been used for DNA sensing[36–39] and the detection of environmental pollutants.[40,41] On the other hand, detection of whole bacterial cells is more difficult and elusive in comparison to gas, liquids, and biomolecules mostly due to the impossibility for bacterial cells ($\approx 1\ \mu m$) to percolate throughout the porous structure. Note that direct detection of whole cells would offer great advantages over other indirect detection schemes as in this case, sensitivity and selectivity are usually higher than indirect methods, i.e., due to the minimization of interferences from exogenous or endogenous analytes. In these regards, Miller and co-workers in a seminal
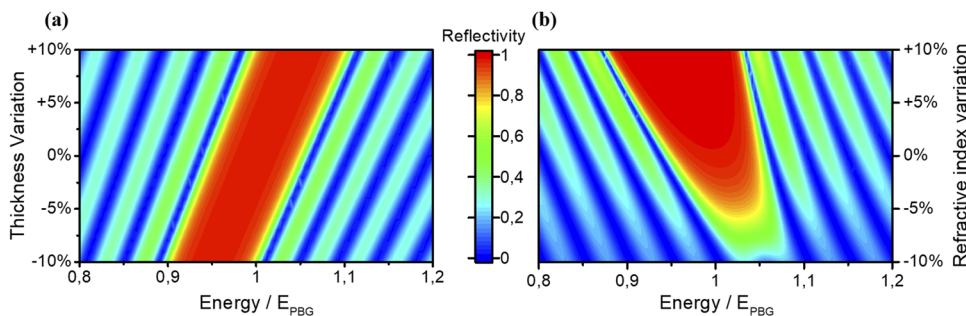
FIG. 2. Color coded reflectivity of an ideal BS responding to the variation of (a) thickness and (b) high refractive index.

work have proposed a PSi resonator functionalized with an organic receptor that specifically binds to the Gram (−) bacterial membrane, observing a red-shift (4 nm) of photoluminescence upon exposure to *Escherichia coli*.[39] A similar PSi microcavity architecture has been employed in a more recent work, in which the authors fabricated a chip for detecting bacteria for the molecular or subcellular analysis by surface modification using undecylenic acid, demonstrating the specific recognition binding of vancomycin to the D-alanyl-D-alanine of bacteria (Fig. 3).[43] In general, these interesting studies demonstrate that PhCs can be effectively used for detecting bacteria and contaminants and hold promises for their employment in food quality control, although the reported spectral shift is by far too low for attaining visual colorimetric recognition of the analytes. Assessing the PSi optical transducer technology, one should note that they have two main advantages: (i) the high refractive index sensitivity, in the order of 1000 nm/refractive index unit, a value that is competitive with more-geometrically complex devices, such as those integrating nanopillars and nanorings;[44] (ii) the easy and low-cost fabrication procedure via controlled electro-chemical dissolution of crystalline silicon at room temperature.[45] Conversely, the main disadvantages of PSi-based optical devices also originate from the electrochemical etching process that is at the core of their fabrication, such as the use of hazardous hydrofluoric acid, the lack of reproducibility of pore size distribution that is essential for analyte percolation, and the reactivity of the highly hydrogenated freshly etched surface, which tends to be substituted by Si–O on exposure to atmospheric oxygen, thus determining a large variability in the optical response. As a final remark, even though PSi-based biosensors have been proposed for the detection of target bacteria of interest for the food

industry,[46] the use of DBRs as simple colorimetric systems for tracking such analytes has not been demonstrated yet, to the best of our knowledge.

An important class of mesoporous DBRs are based on a multilayer of colloidal nanoparticles (NPs) deposited by solution-based wet processes,[48,49] such as sol–gel method, dip-coating, or simple sequential spin-casting of the colloidal dispersion.[50,51] Here, again, responsivity to a large variety of external stimuli is obtained, thanks to the large surface area available for physical and chemical interaction with the analytes. The versatility of fabrication[52] and the possibility to integrate different materials, such as metal oxide NPs (i.e., SiO_2, TiO_2, and SnO_2), clays, zeolites, electrolytes, and liquid crystals,[53,54] have made these DBRs popular in a variety of fields.[51] These include optoelectronics,[55–57] lasing,[58,59] sensing of liquids,[48] and vapors.[60,61] In this latter regards, Ozin and collaborators have pioneered the development of photonic nose-sensors for the control of water and food. This approach relies on the patterning of the DBR surface with different alkoxysilanes to achieve a combinatorial array with distinct surface energy characteristics.[62,63] In the first set of experiments, the authors validate such a method by exposing the DBR arrays to a series of alcohols and alkanes and by calculating the absolute difference between the reference and solvent-exposed DBR images.[62] The response of each specifically functionalized surface has been analyzed using the principal component analysis (PCA). Such a statistical approach allows studying high-dimensionality datasets by reducing the number of variables and finding statistically relevant linear relations among them. This permits us to reduce the number of variables, thus helping to find clusters of data having similar properties.[64] In the case of this work,
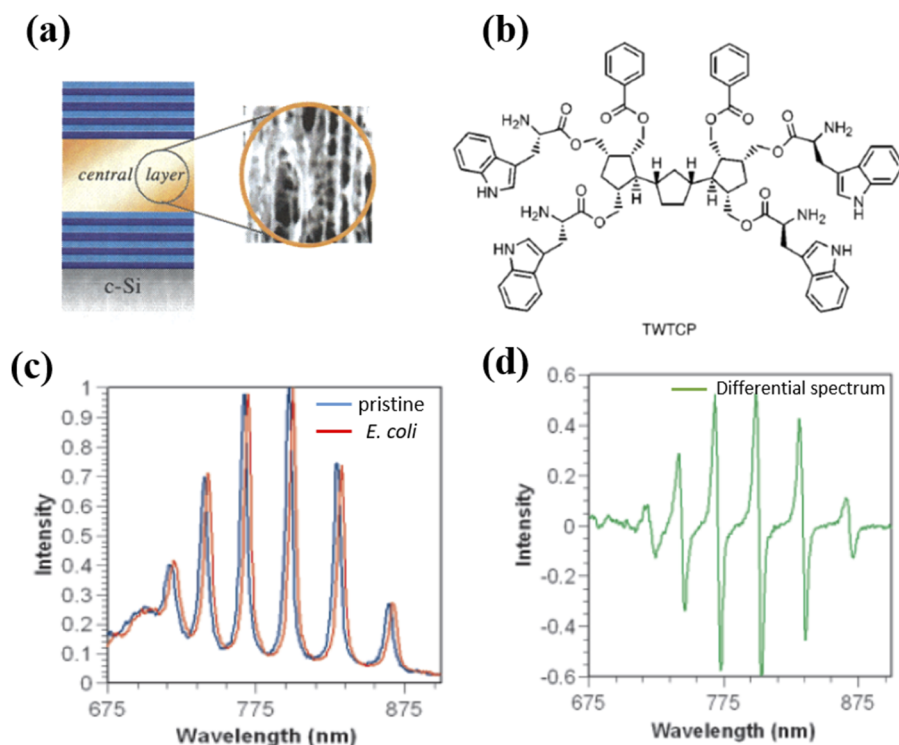
FIG. 3. (a) Sketch of the porous silicon resonator employed in Ref. 42 to detect gram (−) bacteria, in which a central emissive layer is sandwiched between two dielectric mirrors (DBRs). (b) Molecular structure of tetratryptophan ter-cyclo pentane (TWTCP), which specifically binds to diphosphoryl lipid A in water with a dissociation constant of 592 nM.[47] (c) Photoluminescence pattern of a porous silicon microcavity in the absence (blue curve) and presence (red curve) of bacterial cell lysates from gram (−) bacteria (*E. coli*) following derivatization with TWTCP and glycine methyl ester. (d) Difference emission spectra obtained in the presence and absence of bacterial cell lysates. Adapted with permission from Chan *et al.*, J. Am. Chem. Soc. **123**, 11797 (2001). Copyright 2001 American Chemical Society.

PCA revealed a significant degree of discrimination between different alcohols and alkanes [Fig. 4(a)]. Following such a preliminary test, the authors proceeded on the analysis of the volatile compounds produced by different bacterial strains [Fig. 4(b)]. The photonic-nose was unable to distinguish *Pseudomonas aeruginosa* and *Staphylococcus epidermidis*, while the other bacterial strains could be discriminated. In a follow-up study, the same group reported a more comprehensive investigation on the response of the photonic-nose upon exposure to biogenic amines that are important indicators of bacterial proliferation in food [Figs. 4(c) and 4(d)].[65] As a proof-of-concept experiment, the authors monitored the quality of organic salmon and ground beef specimens, observing a clear discrimination between the chemical species originating from the degradation of those food samples. More recently, the concept of photonic-nose has been extended to mesoporous colloidal photonic crystal beads[66] and integrated DBR-light emitting diode devices,[67] indicating that there is still room for improvement for such a technology. However, we reckon that these devices should achieve chemical selectivity and a colorimetric response to be utilized in food industry.

To this end, González-Pedro *et al.* have very recently shown the proof-of-concept of a mesoporous DBR-based biosensor that, thanks to the specific chemical functionalization of the whole DBR volume, can be used for biorecognition purposes.[68] In particular, the authors investigated the biosensor performances by monitoring the optical response of the biotin functionalized porous DBR produced by the selective attachment of streptavidin, observing a colorimetric shift upon the streptavidin–biotin interaction that leads to the modification of the effective refractive index. In addition, the DBR biosensors were also integrated in analytical systems based on the compact disk technology, which has been previously adopted for analytical applications in the food safety sector.[69] This is particularly relevant for future possible applications of mesoporous DBRs in such a field. However, it is worth saying that

such architecture does not allow direct detection of whole bacterial cells.

III. POLYMER DBRs

Polymer (or plastic) photonic crystals have been an object of intense scientific interest, especially in the last couple of decades,[22] due to their simple fabrication from the solution-based process, good mechanical properties, and low interfacial roughness that ensure easy integration of these systems in a variety of devices ranging from microcavities for emission control and lasers[70–73] to light emitting diodes,[74,75] solar cells,[76–78] and sensing.[79] In this latter case, the sensing mechanism is usually connected to the permeability of the polymer materials owing to the free volume between the entangled polymer chains, while selectivity is governed by the affinity of the analyte for the polymer, as described by the Flory–Huggins solution theory[80] and the Hildebrand solubility parameter.[22] Such an effect has been, in fact, exploited to build up colorimetric Flory–Huggins sensors to detect volatile aromatic compounds in a label-free fashion. In these regards, Convertino *et al.* first reported on the detection of organic solvents,[81] although the authors used costly and time-consuming chemical vapor deposition to fabricate the multilayers. Only recently, solution-processed polymer DBRs have been proposed as low-cost optical transducers to monitor environmental pollutants.[82–84] For instance, Lova *et al.* have demonstrated label-free colorimetric detection of aromatic volatile compounds by means of photonic sensors (Fig. 5).[85] In particular, the authors embedded poly(*p*-phenylene oxide) in the polymeric multilayers, in order to exploit its ability to uptake a large amount of guest molecules and form co-crystalline and nanoporous phases with different optical properties. In this way, they were able to discriminate with relatively good selectivity carbon tetrachloride, benzene, and 1,2-dichlorobenzene due to the different ability of the guest
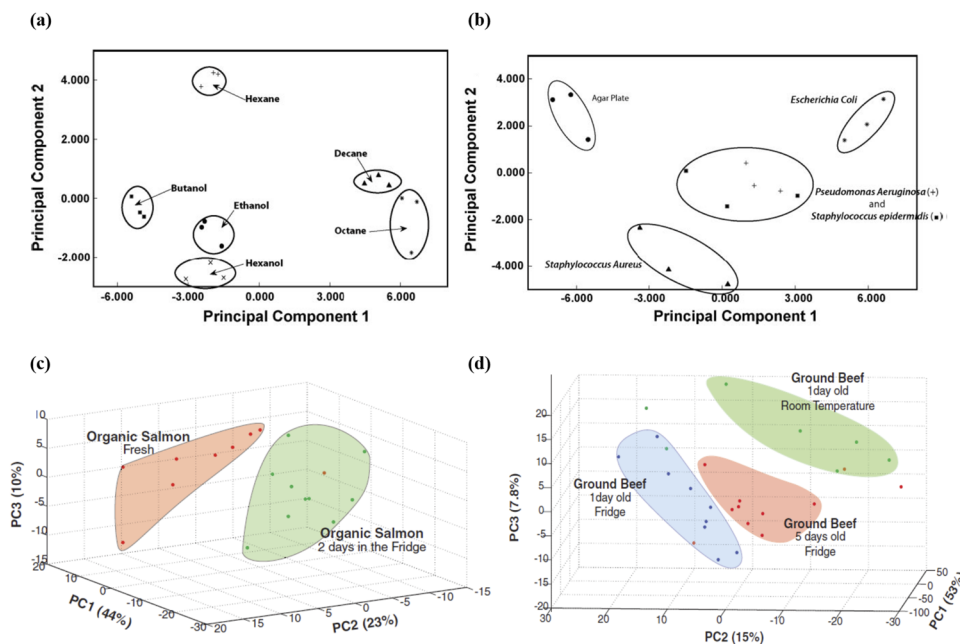
FIG. 4. (a) Principal component analysis of the color changes upon exposure of the photonic-nose array composed of DBRs to different alkanes and alcohols. (b) Principal component analysis of the color changes induced by volatile molecules produced by different bacterial strains. (c) PCA plots for organic salmon and (d) ground beef. Panels (a) and (b) are adapted with permission from Bonifacio *et al.*, Adv. Mater. **22**, 1351 (2010). Copyright 2010 John Wiley and Sons. Panels (c) and (d) are adapted with permission from L. D. Bonifacio, G. A. Ozin, and A. C. Arsenault, Small **7**, 3153 (2011). Copyright 2011 John Wiley and Sons.

FIG. 5. Transmittance spectra of the plastic DBRs composed of cellulose acetate and poly(*p*-phenylene oxide) upon exposure to benzene, 1,2-dichlorobenzene, and carbon tetrachloride as a function of time. Adapted with permission from Lova *et al.*, ACS Appl. Mater. Interfaces **11**, 16872 (2019). Copyright 2019 The American Chemical Society. Further related to the material excerpted should be directed to the ACS.

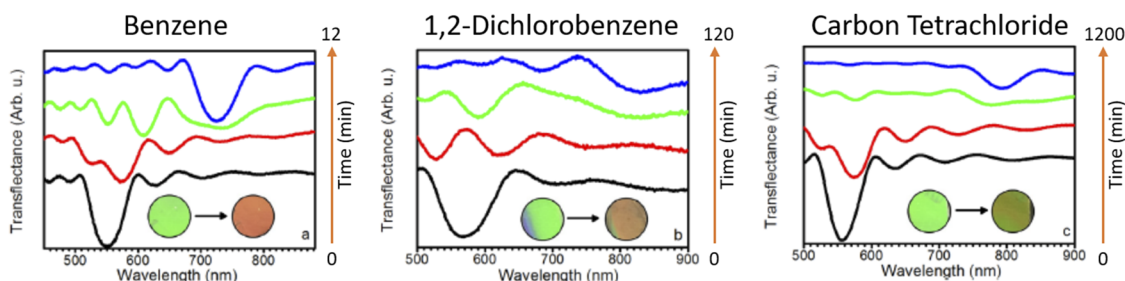molecules to induce co-crystalline and nanoporous crystalline phases in the poly(*p*-phenylene oxide). As is also shown in Fig. 5, the color shift is sufficient to be discriminated using naked eyes.

In the field of biosensing, Olsen and co-workers have shown that DBRs based on a block-copolymer electrolyte gel can be used as a colorimetric sensor for proteins. In particular, the gel layers swell/deswell when the block-copolymer gels are exposed to protein solutions that form coacervates with the polyelectrolyte block, resulting in a variation of the photonic lattice and, hence, the structural color.[86] However, despite these research efforts, plastic DBRs have never been extensively studied as optical biosensors for tracking food contaminants, degradation by-products (i.e., biogenic amines), or whole pathogenic bacterial cells. For the latter case, for instance, this is essentially related to the impossibility for bacterial cells to perturb the free volume in the polymer network, while we reckon that such a detection scheme could be instead applied for the detection of the degradation by-products. The introduction of these systems can be desirable for the food quality sector as polymer DBRs could guarantee the colorimetric response, selectivity, and sensitivities in the ranges of inorganic mesoporous DBRs ($\approx 10^{-1}$ ppm), [31] but probably affording a higher mechanical resilience and conformability.

IV. HYBRID 1D PLASMONIC/PHOTONIC CRYSTALS

The incorporation of plasmonic materials into photonic crystals and, in particular, mesoporous DBRs has recently opened a novel and promising pathway to confer responsivity to these otherwise passive optical elements.[87] With the term plasmons, we refer to the quantized collective oscillations of free electrons in the material that can interact with electromagnetic waves. Each plasmon is characterized by an oscillation frequency called plasma frequency ω_p that is typically included inside the UV/visible/NIR electromagnetic frequency spectrum. The dielectric function of a material having plasmonic resonances sharply changes in proximity of ω_p; the imaginary part rises, and the real part oscillates. The plasma frequency, in turn, responds strongly to changes in the charge carrier density,[88] as expressed by the following equation:

$$\omega_p = \sqrt{\frac{Ne^2}{m^* \varepsilon_0}}, \qquad (4)$$

where N is the charge carrier density, e is the electron charge, ε_0 is the dielectric constant in the vacuum, and m^* is the effective mass, thus meaning that an active control of the frequency dependent dielectric constant $[\varepsilon(\omega) = \varepsilon_1(\omega) + i\varepsilon_2(\omega)]$[89] in plasmonic materials can be achieved via modulation of the charge carrier density. This, interestingly, permits us to modulate the refractive index contrast in PhCs doped with plasmonic materials and, as a consequence, modify the photonic bandgap and the structural color [see Eqs. (1)–(3) in the Introduction]. The first investigation on the integration of plasmonic heavily doped semiconductor nanoparticles in DBRs was reported by Puzzo *et al.* about 10 years ago,[90] although the exploitation of the tunable plasmonic response to modify the overall photonic readout has been demonstrated only recently, i.e., to build up electro-responsive Bragg stacks.[91,92] Within this context, we have reported on the fabrication of electro/optical switches based on the blue-shift of the photonic bandgap caused by photo/electro doping of indium tin oxide (ITO) nanoparticles in SiO$_2$/ITO and TiO2/ITO DBRs[93–95] and electro doping of silver nanoparticles in TiO$_2$/Ag crystals.[96] Furthermore, biosensing capabilities can be enabled for those plasmonic materials that possess a certain bioactivity. Silver, for instance, is a metal showing plasmonic resonances in the Vis/UV whose bactericidal activity is well-recognized, [97] representing, in fact, the first antibacterial system before the discovery of antibiotics in the last century.[98] Such an activity has been connected to the relatively strong electrostatic adhesion between the either the negatively charged bacterial membrane or proteins and the positive silver surface, followed by Ag$^+$ uptake inside the bacterial cells. This finally leads to a series of unfavorable events for bacterial cell viability, such as an increase in membrane permeability and depolarization, interference with the respiratory chain, and production of reactive oxygen species.[99] Our groups have preliminary investigated the effect of the silver/bacterial interaction on the plasma frequency, observing a blue-shift in the plasmon resonance upon bacterial contamination. We attributed this effect to the modification of the carrier density brought about by the strong Ag$^+$/bacterial interaction, within a sort of "bio-doping" mechanism.[95,100] However, other possible concomitant causes, such as modifications of particle size brought about by silver oxidative dissolution[101] and bacterial uptake that might determine appreciable shifts in the plasmon frequency, cannot be completely ruled out. Interestingly, by integrating the plasmonic functionality in the 1D PhC, we have observed that such a plasmon modulation is translated into a photonic readout
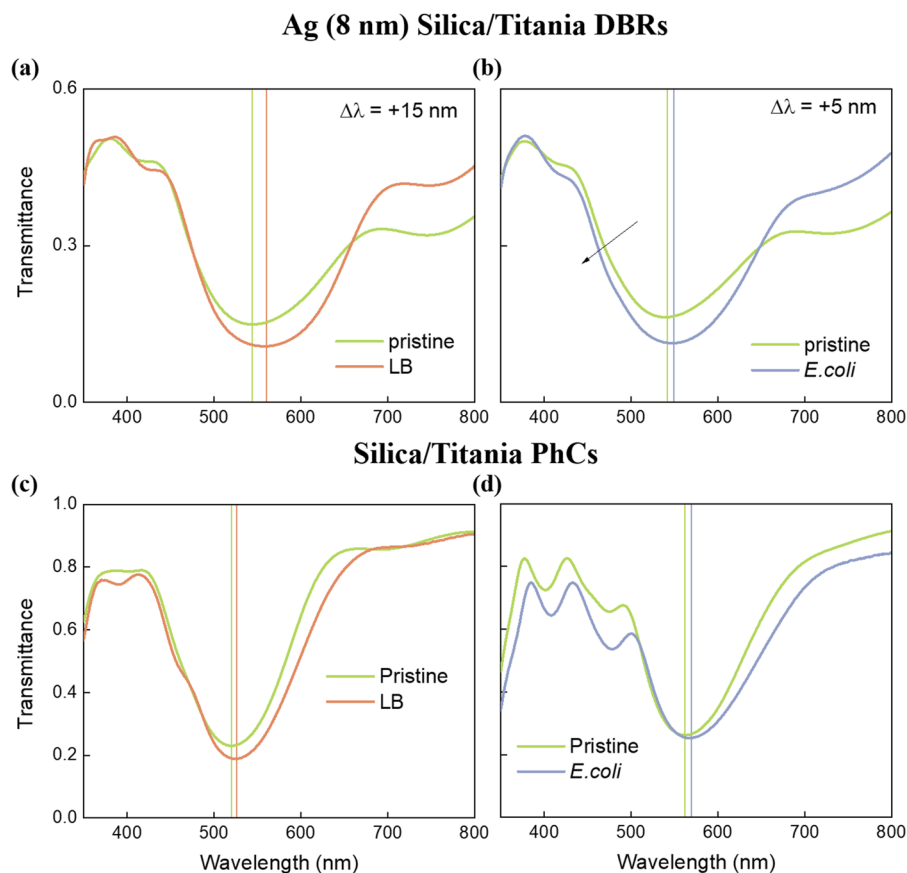
FIG. 6. (a) Transmittance spectrum of Ag/1D photonic crystals upon exposure to the LB medium and (b) *E. coli*. (c) Transmittance spectrum of 1D photonic crystals (without the Ag layer) upon exposure to the LB medium and (d) *E. coli*. Adapted with permission from Paternò *et al.*, J. Phys. Chem. Lett. **10**, 4980–4986 (2019). Copyright 2019 The American Chemical Society.

(Fig. 6). The approach consisted in the exploitation of the possible change in the silver complex dielectric function driven by the Ag/bacterial interaction to modify the dielectric properties at the DBR/metal interface and, thus, the overall DBR transmission spectrum. With this in mind, we first selected the minimum Ag thickness achievable with our deposition apparatus (8 nm) to localize strongly the plasmonic field enhancement in the close proximity to the DBR interface. As a proof-of-concept, we tested the validity of our method by detecting one of the most hazardous contaminants in food and water, namely, *Escherichia coli*. By exposing the hybrid DBRs to either the culture medium (Luria–Bertani broth, LB) or the bacterium, we reported a differential 10 nm blue-shift of the bandgap after exposure to *E. coli* [Figs. 6(a) and 6(b)]. On the other hand, we could not observe any effect on the silica/titanium DBR without the top Ag layer [Figs. 6(c) and 6(d)], indicating that the plasmonic material represents the responsivity element of our hybrid plasmonic–photonic device. However, a precise colorimetric response that would actually denote a clear paradigm shift in the field of bacterial detection was still missing.

In this regard, our group has recently demonstrated some preliminary evidence of colorimetric detection of *E. coli* by optimizing the optical quality of the DBRs in terms of transmittance intensity [Figs. 7(a) and 7(b)]. These devices allow recording an average blue-shift of 30 nm upon microbial contamination that leads to a visual shift of the structural color [Fig. 7(c)]. Furthermore, we extended our investigation to a gram (+) bacterium *Micrococcus luteus*, which is of interest in the poultry industry.[102] In this case, we observed a less obvious photonic shift, an effect that we attributed to the efficient electrostatic interaction and cellular adhesion between the silver surface and the gram (−) bacterial outer membrane.[103]

In summary, such a hybrid plasmonic/photonic approach exploits, in fact, a physical functionalization process that presents two important advantages over chemically modified PhCs, specifically: (i) enhanced environmental stability due to the reduced reactivity of the constituent elements; (ii) scalability, i.e., by using radio-frequency sputtering deposition.[104] In addition, the large library of bio-tunable plasmonic materials, including noble metals, highly doped metal oxide, and nitrides,[91,105,106] could certainly contribute to the development of this field. In order to be applied effectively as low-cost and portable colorimetric sensors, at both the food industry and customer levels, these devices need, however, additional research to improve their selectivity and sensitivity limits.
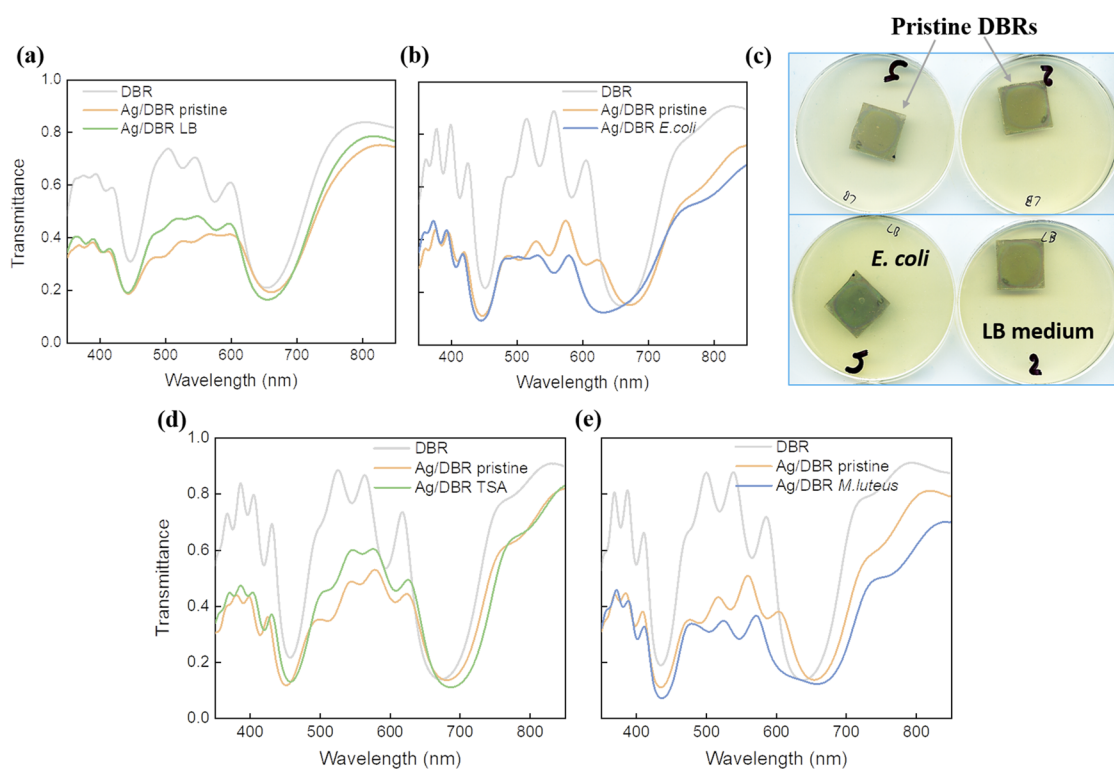
FIG. 7. (a) Transmittance spectra of the DBRs before and after silver deposition and upon exposure to LB and (b) after exposure to *E. coli*. (c) Colorimetric change in the photonic crystals after contamination with *E. coli*, while exposure to LB does not cause any substantial colorimetric change. (d) Transmittance spectra of the DBRs before and after silver deposition and upon exposure to the culture medium [tryptic soy agar (TSA)] and (e) after exposure to *M. luteus*. Reproduced with permisssion from Paternò *et al.*, Faraday Discuss. (to be published) (2020). Copyright 2020 Royal Society of Chemistry.

V. SUMMARY AND DISCUSSION

The huge extension of the food supply chain worldwide can pose severe issues in terms of food quality, an aspect that has recently encouraged a steep development in the field of food quality control. Food degradation concur with a large fraction of food wastage (around 30%), meaning that its minimization is, thus, crucial in our overpopulated world within a circular economy paradigm. Therefore, modern sensors for food quality control should desirably be widespread, portable, and reusable/recyclable and should allow for a rapid detection of the contaminants to minimize the risk of cross-contamination. Here, we showed that photonic crystal-based sensors can, in principle, fulfill these requirements. We briefly introduced the main working principle based on the modification of the dielectric constant in the periodic structure by the presence of the contaminant. The change might stem from the change in density, largest when contrasted by air, or more specifically by the change in polarizability within the bandgap spectral range. Generally, anyway, disruption of the DBR periodicity brings about a change in the optical response. Nature offers a spectacular demonstration of this phenomenon in animal and plant camouflage that is based on the control of the architecture and composition of some attributes, typically the skin, giving rise to structural colors. Aiming at

practical application, both selectivity and naked eye detection, which also allow easy readout by unskilled operators, are crucial. Selectivity can be achieved either by introducing specific biochemical functionalities or via physical matching of the analyte with the periodic cell. In the case of bacteria, however, their size poses challenges for the direct detection of whole cells. Either the resonance frequency falls in the microwave range or there should be a secondary structure finalized for capturing the bacteria, while a fine underneath structure is responsible for the structural color. Most obviously, the effect of the bacteria should necessarily be averaged over many periods of the DBR and rely on interaction at the molecular or ionic level. We showed here that this later approach indeed works with the plasmonic DBR and that strategies to amplify the primary bio-doping up to the naked-eye detection limit can be envisaged in those systems. The low-cost fabrication process is an additional advantage of the DBR approach. Indeed, among the PhCs, DBRs represent the simplest architecture as the structural photonic color arises simply from the periodic alternation of layers with different refractive indices. Despite their intrinsic geometrical simplicity, they exhibit high optical purity and easy integration with a large number of stimulus responsive materials, an aspect that is important to achieve selectivity and sensitivity. In this perspective, we described the main approaches that have been adopted to make DBRs

suitable for the detection of pollutants and bacteria, in view of their application for food and water quality control. In regard to the application in real and complex food matrices, selectivity and sensitivity should be greatly enhanced in DBRs-based sensors, as in real samples, the presence of a plethora of chemicals (i.e., biomacromolecules) can, in principle, lead to the modification of the refractive index contrast and/or on the photonic lattice spacing and, thus, to false positives. This can be solved by judiciously adding specific bio-chemical and physical functionalities to the photonic structure. Enhanced selectivity/sensitivity within a colorimetric detection scheme and the possibility to fabricate reusable and recyclable DRB sensors by means of scalable and low-cost processes are, in fact, the key elements that would permit a widespread use of these devices in real settings, i.e., at the factory and the customers' levels.

Although these systems have not entered the market yet, we reckon that various research groups around the world are addressing the main issues that need to be overcome to bridge the death-valley between the laboratory and the full commercialization of this technology.

ACKNOWLEDGMENTS

DATA AVAILABILITY

The data that support the findings of this study are available from the corresponding author upon reasonable request.

REFERENCES

[1] E. Costell, Food Qual. Preference **13**, 341 (2002).

[2] E. B. Bahadır and M. K. Sezgintürk, Anal. Biochem. **478**, 107 (2015).

[3] F. Mustafa and S. Andreescu, Foods **7**, 168 (2018).

[4] M. V. Vilariño, C. Franco, and C. Quarrington, Front. Environ. Sci. **5**, 21 (2017).

[5] R. A. Neff, R. Kanter, and S. Vandevijvere, Health Aff. **34**, 1821 (2015).

[6] D. Liu, Molecular Detection of Foodborne Pathogens (CRC Press, 2009).

[7] N. Tzamtzis, G. P. Nikoleli, T. Varzakas, D. P. Nikolelis, V. N. Psychoyios, N. Psaroudakis, and S. Liodakis, "Lab-on-a-chip and microfluidic technology," in Portable Biosensing of Food Toxicants and Environmental Pollutants (CRC Press, 2013).

[8] V. Velusamy, K. Arshak, O. Korostynska, K. Oliwa, and C. Adley, Biotechnol. Adv. **28**, 232 (2010).

[9] C. Fenzl, T. Hirsch, and O. S. Wolfbeis, Angew. Chem., Int. Ed. **53**, 3318 (2014).

[10] H. Wang and K.-Q. Zhang, Sensors **13**, 4192 (2013).

[11] S. Vignolini, P. J. Rudall, A. V. Rowland, A. Reed, E. Moyroud, R. B. Faden, J. J. Baumberg, B. J. Glover, and U. Steiner, Proc. Natl. Acad. Sci. U. S. A. **109**, 15712 (2012).

[12] P. Vukusic, J. R. Sambles, and C. R. Lawrence, Nature **404**, 457 (2000).

[13] P. Vukusic and J. R. Sambles, Nature **424**, 852 (2003).

[14] J. H. Nelson, Proc. Phys. Soc. **50**, 661 (1938).

[15] R. A. Potyrailo, H. Ghiradella, A. Vertiatchikh, K. Dovidenko, J. R. Cournoyer, and E. Olson, Nat. Photonics **1**, 123 (2007).

[16] R. A. Potyrailo, R. K. Bonam, J. G. Hartley, T. A. Starkey, P. Vukusic, M. Vasudev, T. Bunning, R. R. Naik, Z. Tang, M. A. Palacios, M. Larsen, L. A. Le Tarte, J. C. Grande, S. Zhong, and T. Deng, Nat. Commun. **6**, 7959 (2015).

[17] R. A. Potyrailo, "Bio-inspired device offers new model for vapor sensing," Proc. SPIE available at https://spie.org/news/3568-bio-inspired-device-offers-new-model-for-vapor-sensing?SSO=1.

[18] L. Nucara, F. Greco, and V. Mattoli, J. Mater. Chem. C **3**, 8449 (2015).

[19] G. M. Paternò, L. Moretti, A. J. Barker, C. D'Andrea, A. Luzio, N. Barbero, S. Galliano, C. Barolo, G. Lanzani, and F. Scotognella, J. Mater. Chem. C **5**, 7732 (2017).

[20] G. M. Paternò, N. Barbero, S. Galliano, C. Barolo, G. Lanzani, F. Scotognella, and R. Borrelli, J. Mater. Chem. C **6**, 2778 (2018).

[21] H. Shen, Z. Wang, Y. Wu, and B. Yang, RSC Adv. **6**, 4505 (2016).

[22] P. Lova, G. Manfredi, and D. Comoretto, Adv. Opt. Mater. **6**, 1800730 (2018).

[23] H. Inan, M. Poyraz, F. Inci, M. A. Lifson, M. Baday, B. T. Cunningham, and U. Demirci, Chem. Soc. Rev. **46**, 366 (2017).

[24] J. D. Joannopoulos, S. G. Johnson, J. N. Winn, and R. D. Meade, Photonic Crystals: Molding the Flow Light, 2nd ed. (Princeton University Press, 2011).

[25] L. Pavesi and P. Dubos, Semicond. Sci. Technol. **12**, 570 (1997).

[26] L. Pavesi, G. Panzarini, and L. C. Andreani, Phys. Rev. B **58**, 15794 (1998).

[27] P. A. Snow, E. K. Squire, P. S. J. Russell, and L. T. Canham, J. Appl. Phys. **86**, 1781 (1999).

[28] V. Mulloni and L. Pavesi, Appl. Phys. Lett. **76**, 2523 (2000).

[29] V. Robbiano, G. M. Paternò, A. A. La Mattina, S. G. Motti, G. Lanzani, F. Scotognella, and G. Barillaro, ACS Nano **12**, 4536 (2018).

[30] M. J. Sailor, ACS Nano **1**, 248 (2007).

[31] C. Pacholski, Sensors **13**, 4694 (2013).

[32] M. M. Orosco, C. Pacholski, G. M. Miskelly, and M. J. Sailor, Adv. Mater. **18**, 1393 (2006).

[33] M. M. Orosco, C. Pacholski, and M. J. Sailor, Nat. Nanotechnol. **4**, 255 (2009).

[34] S. Mariani, V. Robbiano, L. M. Strambini, A. Debrassi, G. Egri, L. Dähne, and G. Barillaro, Nat. Commun. **9**, 5256 (2018).

[35] F. Cunin, T. A. Schmedake, J. R. Link, Y. Y. Li, J. Koh, S. N. Bhatia, and M. J. Sailor, Nat. Mater. **1**, 39 (2002).

[36] S. Chan, P. M. Fauchet, Y. Li, L. J. Rothberg, and B. L. Miller, Phys. Status Solidi (A) **182**, 541 (2000).

[37] L. De Stefano, I. Rendina, L. Moretti, A. M. Rossi, A. Lamberti, O. Longo, and P. Arcari, Proc SPIE **5118**, 305 (2003).

[38] G. Di Francia, V. La Ferrara, S. Manzo, and S. Chiavarini, Biosens. Bioelectron. **21**, 661 (2005).

[39] S. Chan, Y. Li, L. J. Rothberg, B. L. Miller, and P. M. Fauchet, Mater. Sci. Eng. C **15**, 277 (2001).

[40] Z. Gaburro, G. Faglia, C. Baratto, G. Sberveglieri, and L. Pavesi, in Materials Research Society Symposium Proceedings (Materials Research Society, 2001), Vol. 638, p. F1161.

[41] J. Huang, S. Li, Q. Chen, and L. Cai, Sci. China Chem. **54**, 1348 (2011).

[42] S. Chan, S. R. Horner, P. M. Fauchet, and B. L. Miller, J. Am. Chem. Soc. **123**, 11797 (2001).

[43] S. Li, J. Huang, and L. Cai, Nanotechnology **22**, 425502 (2011).

[44] L. De Stefano, Sensors **19**, 4776 (2019).

[45] M. J. Sailor, Porous Silicon in Practice: Preparation, Characterization and Applications (Wiley-VCH Verlag GmbH & Co. KGaA, Weinheim, Germany, 2012).

[46] N. Massad-Ivanir, G. Shtenberg, N. Raz, C. Gazenbeek, D. Budding, M. P. Bos, and E. Segal, Sci. Rep. **6**, 38099 (2016).

[47] R. D. Hubbard, S. R. Horner, and B. L. Miller, J. Am. Chem. Soc. **123**, 5810 (2001).

[48] S. Y. Choi, M. Mamak, G. Von Freymann, N. Chopra, and G. A. Ozin, Nano Lett. **6**, 2456 (2006).

[49] M. C. Fuertes, F. J. López-Alcaraz, M. C. Marchi, H. E. Troiani, V. Luca, H. Míguez, and G. J. A. A. Soler-Illia, Adv. Funct. Mater. **17**, 1247 (2007).

[50] K. M. Chen, A. W. Sparks, H.-C. Luan, D. R. Lim, K. Wada, and L. C. Kimerling, Appl. Phys. Lett. **75**, 3805 (1999).

[51] L. D. Bonifacio, B. V. Lotsch, D. P. Puzzo, F. Scotognella, and G. A. Ozin, Adv. Mater. **21**, 1641 (2009).

[52] O. Sánchez-Sobrado, M. E. Calvo, and H. Míguez, J. Mater. Chem. **20**, 8240 (2010).

[53]L. Moretti, L. Criante, G. Lanzani, S. De Silvestri, G. Cerullo, and F. Scotognella, J. Phys. Chem. C **119**, 23632 (2015).

[54]L. Criante and F. Scotognella, J. Phys. Chem. C **116**, 21572 (2012).

[55]S. Colodrero, A. Mihi, L. Häggman, M. Ocaña, G. Boschloo, A. Hagfeldt, and H. Míguez, Adv. Mater. **21**, 764 (2009).

[56]S. Colodrero, A. Mihi, J. A. Anta, M. Ocaña, and H. Míguez, J. Phys. Chem. C **113**, 1150 (2009).

[57]V. Robbiano, G. M. Paternò, G. F. Cotella, T. Fiore, M. Dianetti, M. Scopelliti, F. Brunetti, B. Pignataro, and F. Cacialli, J. Mater. Chem. C **6**, 2502 (2018).

[58]F. Scotognella, D. P. Puzzo, A. Monguzzi, D. S. Wiersma, D. Maschke, R. Tubino, and G. A. Ozin, Small **5**, 2048 (2009).

[59]D. P. Puzzo, F. Scotognella, M. Zavelani-Rossi, M. Sebastian, A. J. Lough, I. Manners, G. Lanzani, R. Tubino, and G. A. Ozin, Nano Lett. **9**, 4273 (2009).

[60]M. C. Fuertes, S. Colodrero, G. Lozano, A. R. González-Elipe, D. Grosso, C. Boissière, C. Sánchez, G. J. d. A. A. Soler-Illia, and H. Míguez, J. Phys. Chem. C **112**, 3157 (2008).

[61]N. Hidalgo, M. E. Calvo, M. G. Bellino, G. J. A. A. Soler-Illia, and H. Míguez, Adv. Funct. Mater. **21**, 2534 (2011).

[62]L. D. Bonifacio, D. P. Puzzo, S. Breslav, B. M. Willey, A. McGeer, and G. A. Ozin, Adv. Mater. **22**, 1351 (2010).

[63]L. D. Bonifacio, G. A. Ozin, and A. C. Arsenault, Small **7**, 3153 (2011).

[64]I. T. Jollife and J. Cadima, Philos. Trans. R. Soc., A **374**, 20150202 (2016).

[65]A. Önal, Food Chem. **103**, 1475 (2007).

[66]Z. Xie, K. Cao, Y. Zhao, L. Bai, H. Gu, H. Xu, and Z.-Z. Gu, Adv. Mater. **26**, 2413 (2014).

[67]A. T. Exner, I. Pavlichenko, D. Baierl, M. Schmidt, G. Derondeau, B. V. Lotsch, P. Lugli, and G. Scarpa, Laser Photonics Rev. **8**, 726 (2014).

[68]V. González-Pedro, M. E. Calvo, H. Míguez, and Á. Maquieira, Biosens. Bioelectron.: X **1**, 100012 (2019).

[69]A. A. Badran, S. Morais, and Á. Maquieira, Anal. Bioanal. Chem. **409**, 2261 (2017).

[70]F. Scotognella, A. Monguzzi, M. Cucini, F. Meinardi, D. Comoretto, and R. Tubino, Int. J. Photoenergy **2008**, 1.

[71]P. Lova, P. Giusto, F. Di Stasio, G. Manfredi, G. M. Paternò, D. Cortecchia, C. Soci, and D. Comoretto, Nanoscale **11**, 8978 (2019).

[72]G. Manfredi, P. Lova, F. Di Stasio, R. Krahne, and D. Comoretto, ACS Photonics **4**, 1761 (2017).

[73]G. Canazza, F. Scotognella, G. Lanzani, S. De Silvestri, M. Zavelani-Rossi, and D. Comoretto, Laser Phys. Lett. **11**, 035804 (2014).

[74]P. K. Ho, D. S. Thomas, R. H. Friend, and N. Tessler, Science **285**, 233 (1999).

[75]T. Kawase, P. K. H. Ho, R. H. Friend, and T. Shimoda, in *Materials Research Society Symposium Proceedings* (Materials Research Society, 2000), p. BB11.49.

[76]G. Iasilli, R. Francischello, P. Lova, S. Silvano, A. Surace, G. Pesce, M. Alloisio, M. Patrini, M. Shimizu, D. Comoretto, and A. Pucci, Mater. Chem. Front. **3**, 429 (2019).

[77]A. Bozzola, V. Robbiano, K. Sparnacci, G. Aprile, L. Boarino, A. Proto, R. Fusco, M. Laus, L. C. Andreani, and D. Comoretto, Adv. Opt. Mater. **4**, 147 (2016).

[78]J. Yin, D. B. Migas, M. Panahandeh-Fard, S. Chen, Z. Wang, P. Lova, and C. Soci, J. Phys. Chem. Lett. **4**, 3303 (2013).

[79]Y. Kang, J. J. Walish, T. Gorishnyy, and E. L. Thomas, Nat. Mater. **6**, 957 (2007).

[80]P. J. Flory, J. Chem. Phys. **9**, 660 (1941).

[81]A. Convertino, A. Capobianchi, A. Valentini, and E. N. M. Cirillo, Adv. Mater. **15**, 1103 (2003).

[82]P. Lova, Polymers **10**, 1161 (2018).

[83]P. Lova, G. Manfredi, C. Bastianini, C. Mennucci, F. Buatier de Mongeot, A. Servida, and D. Comoretto, ACS Appl. Mater. Interfaces **11**, 16872 (2019).

[84]P. Lova, G. Manfredi, L. Boarino, A. Comite, M. Laus, M. Patrini, F. Marabelli, C. Soci, and D. Comoretto, ACS Photonics **2**, 537 (2015).

[85]P. Lova, C. Bastianini, P. Giusto, M. Patrini, P. Rizzo, G. Guerra, M. Iodice, C. Soci, and D. Comoretto, ACS Appl. Mater. Interfaces **8**, 31941 (2016).

[86]Y. Fan, S. Tang, E. L. Thomas, and B. D. Olsen, ACS Nano **8**, 11467 (2014).

[87]S. S. K. Guduru, I. Kriegel, R. Ramponi, and F. Scotognella, J. Phys. Chem. C **119**, 2775 (2015).

[88]J. M. Luther, P. K. Jain, T. Ewers, and A. P. Alivisatos, Nat. Mater. **10**, 361 (2011).

[89]P. Drude, Ann. Phys. **312**, 687 (1902).

[90]D. P. Puzzo, L. D. Bonifacio, J. Oreopoulos, C. M. Yip, I. Manners, and G. A. Ozin, J. Mater. Chem. **19**, 3500 (2009).

[91]S. Heo, A. Agrawal, and D. J. Milliron, Adv. Funct. Mater. **29**, 1904555 (2019).

[92]E. Redel, J. Mlynarski, J. Moir, A. Jelle, C. Huai, S. Petrov, M. G. Helander, F. C. Peiris, G. von Freymann, and G. A. Ozin, Adv. Mater. **24**, OP265 (2012).

[93]G. M. Paternò, C. Iseppon, A. D'Altri, C. Fasanotti, G. Merati, M. Randi, A. Desii, E. A. A. Pogna, D. Viola, G. Cerullo, F. Scotognella, and I. Kriegel, Sci. Rep. **8**, 3517 (2018).

[94]G. M. Paternò, L. Moscardi, I. Kriegel, F. Scotognella, and G. Lanzani, J. Photonics Energy **8**, 1 (2018).

[95]F. Scotognella, G. M. Paternò, I. Kriegel, S. Bonfadini, L. Moscardi, L. Criante, S. Donini, D. Ariodanti, M. Zani, E. Parisini, and G. Lanzani, "Ultrafast photochromism and bacteriochromism in one dimensional hybrid plasmonic photonic structures," Proc SPIE **11357**, 113571G (2020).

[96]E. Aluicio-Sarduy, S. Callegari, D. G. F. del Valle, A. Desii, I. Kriegel, and F. Scotognella, Beilstein J. Nanotechnol. **7**, 1404 (2016).

[97]B. Le Ouay and F. Stellacci, Nano Today **10**, 339 (2015).

[98]K. Mijnendonckx, N. Leys, J. Mahillon, S. Silver, and R. Van Houdt, BioMetals **26**, 609 (2013).

[99]L. Rizzello and P. P. Pompa, Chem. Soc. Rev. **43**, 1501 (2014).

[100]G. M. Paternò, L. Moscardi, S. Donini, D. Ariodanti, I. Kriegel, M. Zani, E. Parisini, F. Scotognella, and G. Lanzani, J. Phys. Chem. Lett. **10**, 4980–4986 (2019).

[101]K. B. Mogensen and K. Kneipp, J. Phys. Chem. C **118**, 28075 (2014).

[102]W. Laba, A. Choinska, A. Rodziewicz, and M. Piegza, Braz. J. Microbiol. **46**, 691 (2015).

[103]G. M. Paterno, L. Moscardi, S. Donini, A. M. Ross, S. M. Pietralunga, N. Dalla Vedova, S. Normani, I. Kriegel, G. Lanzani, and F. Scotognella, Faraday Discuss. (published online, 2020).

[104]F. Scotognella, A. Chiasera, L. Criante, E. Aluicio-Sarduy, S. Varas, S. Pelli, A. Łukowiak, G. C. Righini, R. Ramponi, and M. Ferrari, Ceram. Int. **41**, 8655 (2015).

[105]A. Llordés, G. Garcia, J. Gazquez, and D. J. Milliron, Nature **500**, 323 (2013).

[106]R. J. Mendelsberg, P. M. Mcbride, J. T. Duong, M. J. Bailey, A. Llordes, D. J. Milliron, and B. A. Helms, Adv. Opt. Mater. **3**, 1293 (2015).